Biomed Microdevices (2012) 14:829–838
DOI 10.1007/s10544-012-9662-7

Three-dimensional scaffolding to investigate neuronal derivatives of human embryonic stem cells

Pranav Soman · Brian T. D. Tobe · Jin Woo Lee · Alicia M. Winquist · Ilyas Singec · Kenneth S. Vecchio · Evan Y. Snyder · Shaochen Chen

Published online: 6 July 2012

Abstract Access to unlimited numbers of live human neurons derived from stem cells offers unique opportunities for *in vitro* modeling of neural development, disease-related cellular phenotypes, and drug testing and discovery. However, to develop informative cellular *in vitro* assays, it is important to consider the relevant *in vivo* environment of neural tissues. Biomimetic 3D scaffolds are tools to culture human neurons under defined mechanical and physicochemical properties providing an interconnected porous structure that may potentially enable a higher or more complex organization than traditional two-dimensional monolayer conditions. It is known that even minor variations in the internal geometry and mechanical properties of 3D scaffolds can impact cell behavior including survival, growth, and cell fate choice. In this report, we describe the design and engineering of 3D synthetic polyethylene glycol (PEG)-based and biodegradable gelatin-based scaffolds generated by a free form fabrication technique with precise internal geometry and elastic stiffnesses. We show that human neurons, derived from human embryonic stem (hESC) cells, are able to adhere to these scaffolds and form organoid structures that extend in three dimensions as demonstrated by confocal and electron microscopy. Future refinements of scaffold structure, size and surface chemistries may facilitate long term experiments and designing clinically applicable bioassays.

Keywords 3D scaffolds · Human neurons · Polyethylene glycol · Gelatin methyacrylate

Pranav Soman and Brian T. D. Tobe contributed equally to this work.

P. Soman · J. W. Lee · K. S. Vecchio · S. Chen
Department of NanoEngineering, University of California, San Diego,
9500 Gilman Drive, Atkinson Hall, MC-0448,
La Jolla, CA 92093, USA

B. T. D. Tobe · A. M. Winquist · I. Singec · E. Y. Snyder (✉) · S. Chen
Program in Stem Cell & Regenerative Biology,
Sanford-Burnham Medical Research Institute,
La Jolla, CA 92037, USA
e-mail: esnyder@sanfordburnham.org

B. T. D. Tobe · S. Chen (✉)
Department of Psychiatry, University of California-San Diego,
La Jolla, CA, USA
e-mail: chen168@ucsd.edu

1 Introduction

Human brain microenvironments are highly complex, three-dimensional (3D) structures involving organized interaction of multiple neural cell types with microglia and endothelial cells of the vasculature. Aberrant development, for instance of the cerebral cortical layers, is associated with neurodevelopmental and cognitive disorders (Kunze et al. 2011; Manzini and Walsh 2011). Unlike studies of rodent neural lineages which have been aided by the development of methods for primary culture (Ren and Miller 2003; Silva et al. 2006; Sango et al. 2006), such direct tissue access is generally precluded in studying human neurons providing major obstacles to *in vitro* laboratory models of human neurological diseases. As an alternative, human embryonic stem (hES) cells can be exploited to generate large numbers of neurons *ex vivo*. Recently, progress has been made in directing differentiation of hES cells into the neural stem cells (NSCs) (Chambers et al. 2009; Li et al. 2011; Elkabetz et al. 2008). When grown in suspension, the NSCs can form free-floating cell aggregates, the so-called neurospheres. Eventual plating and adhesion of neurospheres on neurogenic extracellular matrices facilitates neuronal differentiation and

neurite outgrowth (Jensen and Parmar 2006; Deleyrolle and Reynolds 2009). Though directed differentiation strategies for more homogenous neuronal subtypes may be preferable for focused investigations (Perrier et al. 2004; Lee et al. 2007; Zhang 2006; Liu and Zhang 2011), spontaneous heterogeneous differentiation via neurosphere intermediates is often employed owing to practical considerations of minimizing labor and excessive cost required of lengthy directed protocols requiring daily supplementation of numerous exogenous factors and recombinant proteins. In addition, neurospheres themselves have been routinely utilized as an early approximation of neural cellular physiology for various *in vitro* assays (Marshall et al. 2007). However, despite a 3D structure, neurospheres are unstable and highly variable in size, exhibiting frequent remodeling and fusing (Singec et al. 2006). Moreover, both monolayer differentiation and standard neurosphere-based differentiation after plating on substrates inherently impacts neuronal connectivity and may alter kinetics of uptake of nutrients and chemicals, with particular relevance to testing of novel therapeutics.

Though it is as yet unclear how *in vitro* neuronal function might be altered by varying cell culture platforms, one possibility for improving the physiological relevance of human neuronal culture models is the incorporation of 3D scaffolds. Conventional fabrication methods for 3D scaffolds for cell and tissue culture applications are not well-suited for precise control of pore size, pore geometry and spatial distribution or construction of internal channels within the scaffold. (Lee et al. 2008). Diverse cell types have been cultured on various 3D matrices, such as collagen (Ma et al. 2004), fibrin (Willerth et al. 2006) and poly(lactic-coglycolic acid) (Levenberg et al. 2003). More recently, several studies have been reported on the effects of electrospun fibers of a variety of biomaterials including polyamide (Shahbazi et al. 2011), poly(l-lactic acid) (PLLA) (Lam et al. 2011); Yang et al. 2005, poly(l-lactide-co-glycolide) (PLGA) (Bini et al. 2006) and polyurethane (Björn Carlberg et al. 2009) as scaffold surfaces to support stem cell growth and neural differentiation. However, neuronal cells typically adhere to the surface of electrospun scaffolds with minimal penetration. Examination of cell behavior and functional response has proven considerably more challenging largely due to randomly oriented fibers or heterogeneous internal micro-architecture. Changes in the local fiber stiffness in these randomly-oriented fibrous scaffolds results in concurrent changes in biophysical parameters including pore size, fiber architecture and deformability (Storm et al. 2005; Chandran and Barocas 2006; Pedersen and Swartz 2005). Not surprisingly, it has been demonstrated that, in case of 3D fibrous scaffolds (Winer et al. 2009; Gelse et al. 2003; Pathak and Kumar 2011), bulk measurements are considerably less predictive of cell behavior. Internal geometry or micro-architecture plays a vital role in cell behavior and consistent structure inside the scaffold must be maintained to extract reliable data from differentiated cells *in vitro*.

In this work, we present 3D scaffolds with precise internal architecture to investigate neuronal derivatives of human embryonic stem cells using soft and stiff non-biodegradable PEGDA and biodegradable gelatin-based biomaterials scaffolds in either log-pile or hexagonal internal architecture. Previously, we have developed a digital micro-mirror device based projection printing (DMD-PP) system, which can fabricate a 3D scaffold with complex internal geometries in a layer-by-layer fashion by projecting a "photomask" or a "dynamic pattern" on a photocurable monomer (Han et al. 2008; Fozdar et al. 2011; Soman et al. 2012). These scaffolds provide a more controlled environment for isolation and serial study of specific cellular response to design parameters such as elastic stiffness, shape, size and structure. We hypothesized that scaffolds fabricated by DMD-PP with precise and consistent internal architecture may support growth and maintenance of neurons generated from human pluripotent stem cells. Such designer scaffolds, have the potential for a more reproducible and physiologically relevant milieu and will potentially support high-throughput and large-scale applications such as proteomics, metabolomics and high-content screening.

2 Materials and methods

2.1 Hydrogel prepolymer preparation—Poly (ethylene glycol) diacrylate (PEGDA) synthesis

PEGDA, (mol. wt. = 700 kDa), acrylic acid (AA), and 2,2,6,6-tetramethylpiperidine 1-oxyl (TEMPO, free-radical quencher) were purchased from Sigma-Aldrich and used as received. Photoinitiator Irgacure 2959 and TINUVIN 234 UV-dye were obtained from Ciba Chemistry. TINUVIN 234, a UV-absorbing agent, was used to reduce the curing depth of the monomers and adjust the thickness of the microstructures in the DMD-PP fabrication process. TEMPO was used to enhance the contrast of the UV-curing process and optimizes feature resolution at the projection plane. Irgacure 2959 [1 % (w/v)], TINUVIN 234 [0.1 % (w/v)], and TEMPO [0.01 % (w/v)] were added to the PEGDA monomer [19 % (w/v) PEGDA is referred to as soft PEGDA, while 95 % (w/v) PEGDA is referred to as stiff PEGDA) and mixed thoroughly.

2.2 Hydrogel prepolymer preparation - Gelatin methacrylate (GelMA) synthesis

Biodegradable GelMA was formulated as described previously (Gauvin et al. 2012). Briefly, porcine skin gelatin

(Sigma Aldrich, St. Louis, MO, USA) was mixed at 10 % (w/v) into phosphate buffered saline (PBS; Gibco, Billings, MT, USA) at 60 °C. Methacrylic anhydride (MA; Sigma) was added to the solution, stirred for 1 hour at 50 °C, diluted with PBS, and dialyzed against distilled water for one week at 40 °C to remove the unreacted groups from the solution. Synthesized GelMA solution was frozen at −80 °C and lyophilized in a freeze dryer until further usage. Freeze dried GelMA macromer was mixed into PBS (15 % concentration) and stirred at 60 °C until fully dissolved and Irgacure 2959 (1 %(w/v), UV absorber (0.1 % (w/v) HMBS, (2-hydroxy-4-methoxy-benzphenone-5-sulfonic acid), Sigma) and solution quencher (0.01 % (w/v), TEMPO, Sigma) were added to the solution.

2.3 Scaffold fabrication method

To fabricate the scaffold, we have developed a DMD-PP apparatus for rapidly prototyping 3D microstructures (Fig. 1a). The system fabricates 3D architectures through UV polymerization using dynamic pattern generator in which microstructures are developed layer-by-layer from a photo-polymerizable prepolymer. Briefly, a digital light processing (DLP) chip set (1920 × 1080 Discover 4000, Texas Instrument) was used to create active, reflective dynamic photo masks using a uniform UV light source. These photo mask patterns make cross-sectional images of a 3D microstructure and project the patterns onto a photocurable monomer (Fig. 1b). A UV-grade optical lens projects the patterns onto a fabrication stage located at the focus of the projection lens and creates a 3D microstructure layer-by-layer by UV polymerization of the prepolymer layer. After the fabrication of each layer, the Z axis of the fabrication stage was repositioned to create a new layer. A glass coverslip was placed above the microstructure to control the thickness of each microstructure layer. The bottom surface of the coverslip was coated with a nonstick layer formed by Krytox 157 FSH oil (DuPont, Wilmington, DE), which readily releases the cured microstructure. After fabrication, the scaffold was detached from the substrate and washed using DI water.

2.4 Mechanical properties

Scaffold samples of the PEGDA polymer were stored prior to testing in a solution of Isopropyl alcohol (IPA). The samples were decanted and their length and width were measured. The samples were cut into tall, right regular

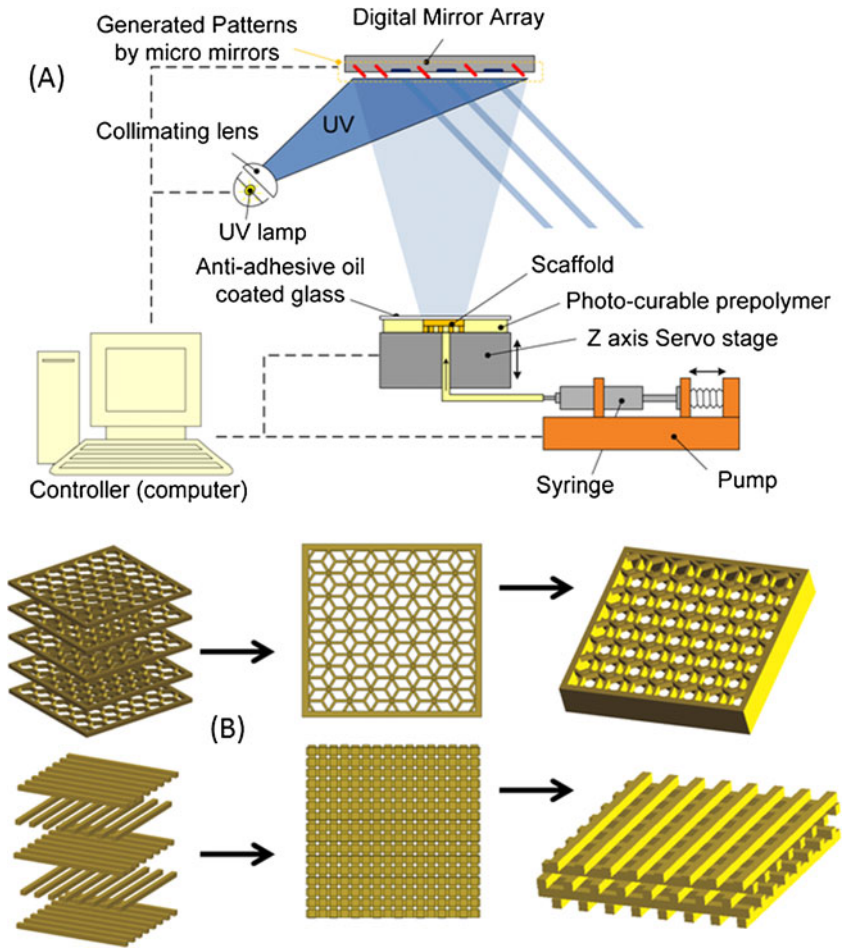

Fig. 1 (**a**) Schematic of the digital micromirror device based projection printing system (DMD-PP) used for fabricating multi-layer biomaterial scaffolds having log-pile and hexagonal internal architectures. The DMD-PP method produced precise features using a system of dynamic masks generated by a digital light controlling chip and photocurable biomaterials. (**b**) Schematic of the assembled structures; the layers of cross-linked photo-polymer can be stacked to form scaffolds having log-pile and hexagonal micro-architecture

prisms (3 mm×3 mm×1 mm) and mounted in a Perkin Elmer thermomechanical analyzer (TMA 7) instrument. The TMA was setup to perform a static force scan, using two 20 mm circular parallel plates. The sample was then loaded with an initial force of 10 mN, and the sample height was determined by Linear Voltage Displacement Transducers (LVDT) of the instrument. During the test, the force was increased on the sample from the initial one (usually 10 mN) to the final force (usually 2500 mN) at a constant rate of 120 mN/min. The initial loading portion of each stress–strain curve was used to determine the modulus of the samples. Typically, 3 samples were tested for each sample type to generate reproducible results. Low-strain and high-strain moduli were defined as the slope of the linear portion of the stress–strain curve comprised between 0–5 % and 10–15 % strain respectively (Fig. 2a,b). Stress–strain curves were plotted and analyzed to facilitate the calculation of the testing parameters. Statistical significance was determined with ANOVA (MINITAB V 14.2, Minitab Inc.), using a standard $p<0.05$.

2.5 Cell culture

PEGDA scaffolds were activated by incubating them in a working solution of 0.15 M 1-ethyl-3-[3-dimethylaminopropyl] carbodiimide hydrochloride (EDC) and 0.12 MN-hydoxysuccinimide (NHS) in 2-[morpholino]ethanesulfonic acid (MES) buffer at pH 5 for 2 hours. PEDGA scaffolds were briefly rinsed with PBS (pH 7.4) to remove any residual NHS and EDC and placed in 96-well plates (one per well) and coated with geltrex (Invitrogen) overnight. GelMA scaffolds were simply coated with geltrex overnight. Human H9 ESC cells were grown on matrigel in MEF-CM with FGF2, differentiated to neural stem cells (NSCs) over 1 week by small molecule mediated induction according to Liu et al. or variation of Chambers et al. (2009; Li et al. 2011). NSCs were mechanically passaged into free floating aggregates and maintained in solution on low attachment plates as neurospheres in DMEM:F12+glutamax with N2B27(Gibco) and penicillin/streptomycin media.

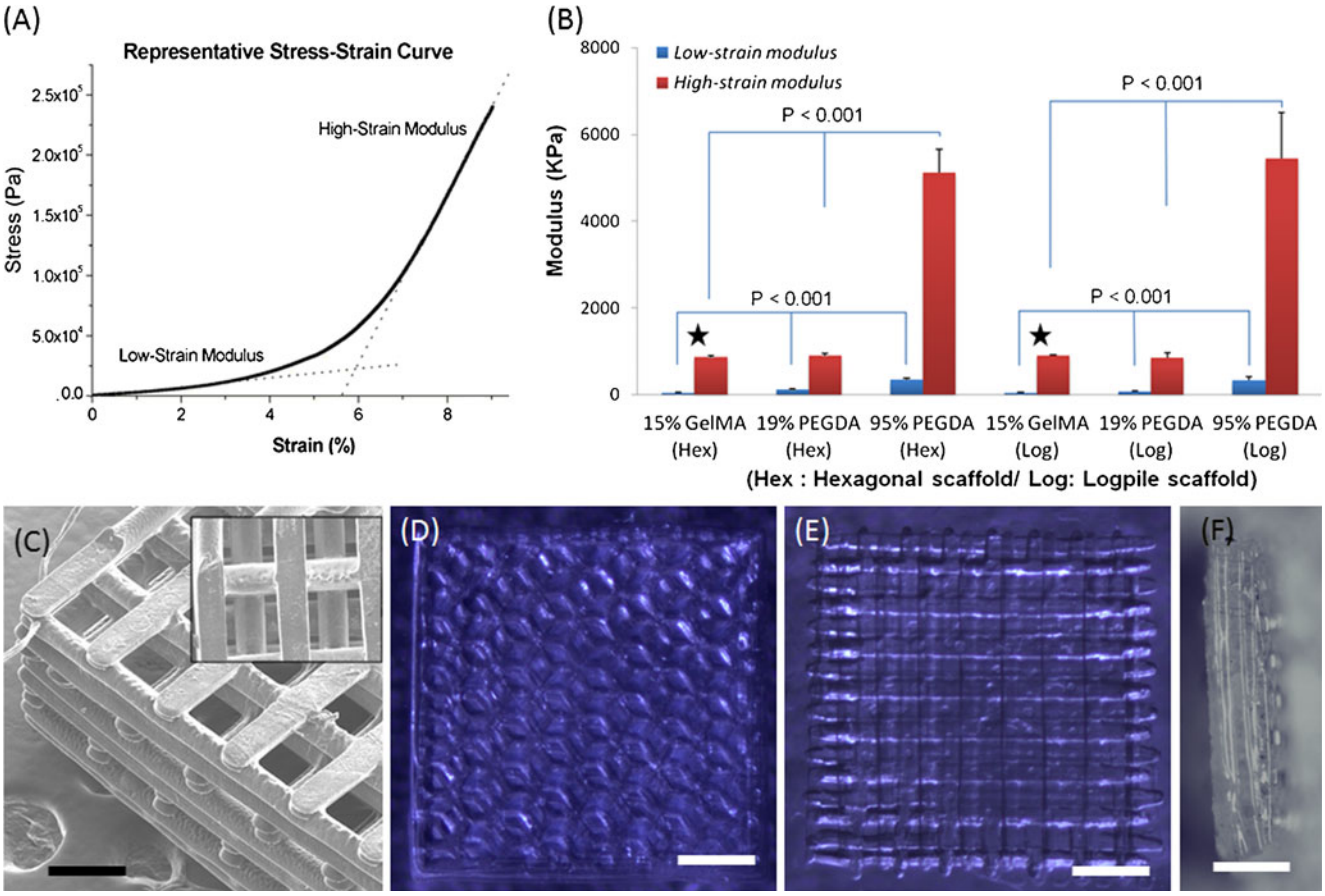

Fig. 2 Mechanical properties of DMD-PP fabricated scaffolds having 3D log-pile and hexagonal structures using soft (19 %) PEGDA, stiff (95 %) PEGDA and gelatin methyacrylate (GelMA). (**a**) A characteristic stress–strain curve displaying low strain and high strain compressive moduli was obtained for every sample tested (**b**) Comparison of compressive modulus of various scaffolds at low and high strains. (**c**) Magnified angled SEM demonstrates the 3D log-pile scaffold. Inset depicts the top-view of the scaffold with precise pore geometries and sharp features. (**d**, **e**) Optical images of log-pile and hexagonal scaffolds (**f**) Side-view of 3D scaffolds showing a 5-layer structure. Black star denotes that the stiffness values are adapted from our earlier work (Gauvin et al. 2012). Scale: C=100 μm; D-F=500 μm

Neurosphere suspensions were either directly transferred to geltrex-coated scaffolds or first plated on geltrex monolayer for differentiation to neurons. Neurosphere suspensions directly transferred to geltrex-coated scaffolds were allowed to attach, then media changed every other day for 3 weeks until cells of neuronal morphology spread from the adherent neurospheres. For neuronal differentiation, neurosphere suspensions were transferred to 6-well plates pre-coated with geltrex (Invitrogen). Cells were allowed to attach, and DMEM:F12+glutamax with N2B27(Gibco) and penicillin/streptomycin media was replaced every other day for 3 weeks until cells showed distinct neuronal morphology. Neurons were subsequently passaged with accutase detachment, washing and transfer to 96 well plates containing scaffolds. Passaged neurons plated on scaffolds were cultured in DMEM:F12+glutamax with N2B27 (Gibco) and penicillin/streptomycin media replaced every other day.

2.6 Scanning electron microscopy

Scanning electron microscopy SEM) was used to analyze the structure of both hESC-derived neurospheres and passaged neurons on the 3D scaffolds. The PEG scaffolds were fixed with glutaraldehyde, and dehydrated in a series of ethanol baths. The specimens were then mounted on stubs and sputter coated with 8 nm thick Iridium using Emitech K575X. The samples were then examined in the Field Emission Environmental scanning electron microscope, FEI XL30 ESEM FEG operated at 10 kV using high vacuum mode.

2.7 Confocal microscopy

Cells were fixed in 4 % PFA, blocked in 3 % BSA solution, incubated with primary rabbit anti- Tuj1 (1:200, Covance MRB-435P), rabbit Map2 (Millipore AB5622, 1:100 dilution) washed, incubated with secondary Alexa Fluor 555 donkey anti-rabbit IgG (1:5000, Invitrogen), and examined with the Olympus Fluoview FV500 software (Olympus). Consecutive confocal images were acquired with optical sections of 0.5 microns for the 0.3 mm-thick central region of the hydrogel. Stack images were constructed from approximately 50 individual optical sections.

3 Results and discussion

3.1 Scaffold fabrication

In this study, we created scaffolds of different internal pore architectures and using two biomaterials that show 5 layer (~100 μm thickness per layer) log-pile and hexagonal shapes as shown in Fig. 1b. Poly(ethylene) glycol (PEGDA) prepolymer concentration of 19 % and 95 % (700 kDa molecular weight) are referred to as soft and stiff PEGDA scaffolds respectively while gelatin methyacrylate scaffolds are referred as GelMA. The UV exposure time was 5 s for stiff PEGDA samples, while 12 s for soft PEGDA and GelMA samples with an UV intensity of 50 mW/cm^2. SEM and optical images of fabricated stiff PEGDA scaffolds depicted in Fig. 2c–f, demonstrate precise fabrication of log-pile and hexagonal structures according to the design files. For the woodpile scaffold, the length of the gap between struts was 250~300 microns, whereas for hexagonal scaffolds, the pore size is approximately 320–340 microns. For soft PEGDA and GelMA samples, SEM imaging led to significant deformation of structure; however optical images were similar to stiff PEGDA (Figs. 2d–f, 6f). The design parameters were chosen to provide increased surface area to support attachment of neuronal process.

3.2 Mechanical properties

The mechanical properties of the scaffolds were measured in order to investigate the influence of pore architecture and different biomaterials used, on the compressive modulus of the microfabricated structures. PEGDA prepolymer concentrations of 19 % and 95 % (700 kDa molecular weight) were used. The compressive response of the porous scaffolds was found to be similar for every sample tested. A biphasic stress–strain relationship comprised of a low strain (0–4 %) and a high strain (8–15 %) response was observed for all 3D scaffolds (Fig. 2a). The low-strain response is a result of the realignment and the reorganization of the struts during the first phase of compression. The low-strain modulus was found to be similar for both log-pile (~47kPa) and hexagonal (~44kPa) GelMA scaffolds, while a slight increase for the soft PEGDA scaffolds for both shapes (log-pile~67kPa; hexagonal ~126kPa) (Fig. 2b). The low-strain responses of the stiff PEGDA scaffold for log-pile and hexagonal geometries are 338kPa and 340kPa respectively. The high-strain response was initiated at a strain level where struts reorganization becomes difficult, an effect of the close packing of porous structure. High strain modulus for both GelMA and soft PEGDA was in a narrow range between 847kPa and 895kPa for both hexagonal and log-pile structures. For the stiff PEGDA scaffolds, the compressive modulus was ~5443 kPa (log-pile) and ~5118kPa hexagonal, significantly higher than those of both GelMA and soft PEGDA scaffolds. These results demonstrate the capability of the DMD-PP method to create 3D scaffolds with complex 3D

internal architectures using both synthetic PEGDA and naturally-derived GelMA biomaterials.

3.3 Effect of scaffold shape and mechanical properties on neurosphere distribution, adhesion and neuronal morphology

To test if scaffolds support neurosphere attachment and differentiation, neurosphere suspensions derived from H9 hESCs were transferred to wells containing scaffolds pre-coated with geltrex. The neurospheres adhered to both log-pile and hexagonal stiff PEGDA scaffolds. SEM micrographs were acquired of neural cells after 21 days of maturation (Fig. 3a–f). Spheres cultivated on both log-pile and hexagonal geometries maintained their 3D organization and developed long-distance neural projections and networks. Interestingly, hexagonal scaffolds facilitated a more even arrangement of neurospheres at least excluding excessively large aggregates (Fig. 3c–f). Though limitations of mass transfer in the interior of the scaffold may prevent stringent homogenous distribution, such gating of neurospheres is largely precluded during plating onto 2D surfaces, which has encumbered reproducible plating density well-known to affect differentiation (Fig. 3f). Conversely, log-pile scaffolds did not demonstrate homogenous size or density distribution. Neurospheres adherent to both log-pile and hexagonal scaffolds showed formation and spreading of neuronal projections in three dimensions indicative of differentiating neurons and apparent intercellular connections as seen in Fig. 3a–f). SEM examination indicated good compatibility with the 3D geometry and topographical sensing, with cross-talk between neighboring cells. These cells were immunoreactive for Tuj1, a neuronal class III beta-tubulin used as a marker of early neurons (Fig. 3g–i). For the log-pile scaffolds, a cell aggregate would attach itself towards the edge/side of the scaffold (Fig. 3h). Neural cells follow the log-pile structure towards the center of the scaffold. With hexagonal geometry, most of the cells aggregate inside the structure forming neurite connections in 3D (Fig. 3i).

We also investigated if PEGDA scaffolds would allow formation of 3D lattices with fewer large cell clusters imparted by neurospheres. Toward examining this possibility, we first plated neurospheres in monolayer on geltrex-coated plates until the cells showed neuronal morphology with 2D intercellular projections. Following detachment with Accutase, these cells were passaged to PEGDA (stiff and soft) and GelMA scaffolds in 96-well plates. After culture for 3 additional weeks, neuronal projections formed 3D networks visible by confocal microscopy on stiff PEGDA scaffolds (Fig. 4). As with direct neurosphere plating and differentiation, cell bodies of passaged neuronal progeny attached to the scaffold surface and extended neural processes both along

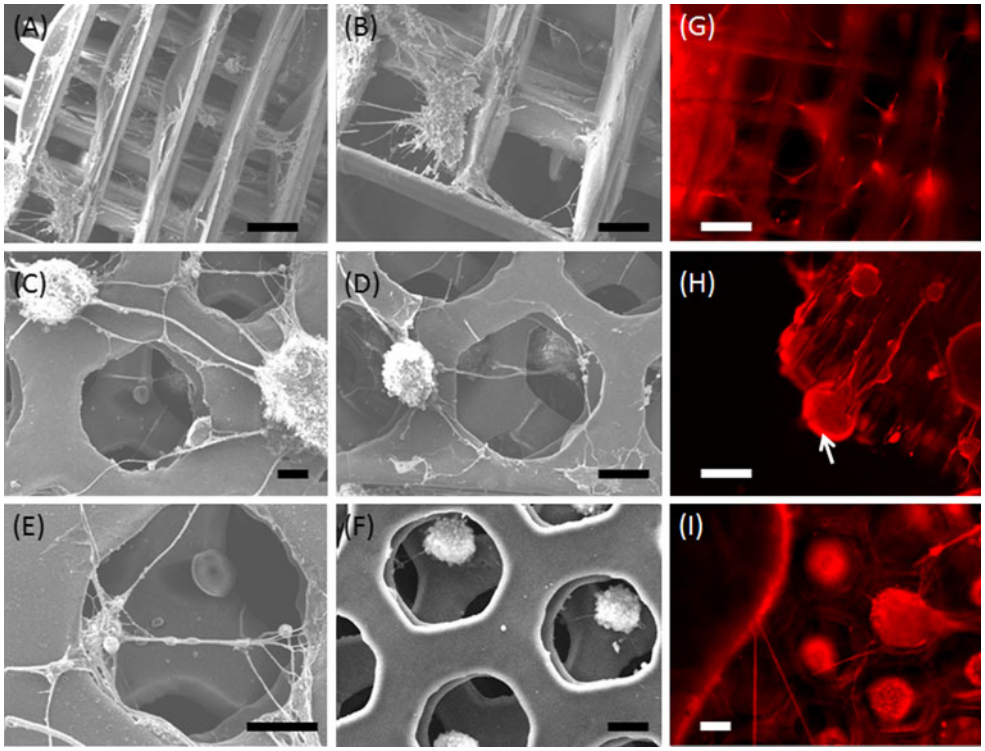

Fig. 3 SEM images of PEG scaffolds with (**a**, **b**) log-pile and (**c**–**f**) hexagonal internal architecture support survival and transition of neurospheres to neuronal morphology, spreading from adherent cell clusters, and forming 2D and 3D intercellular projections. Neurospheres evenly penetrate and adhere to hexagonal PEGDA scaffolds. Larger neurospheres are largely excluded from the interior of the scaffold. (**g**–**i**) Neurons form 3D lattices on log-pile and hexagonal PEGDA scaffolds labeled for Tuj1. White arrow in (**h**) denotes a cell cluster adhered to the side of the log-pile scaffold with neural connections along the struts. Scale: 100 μm

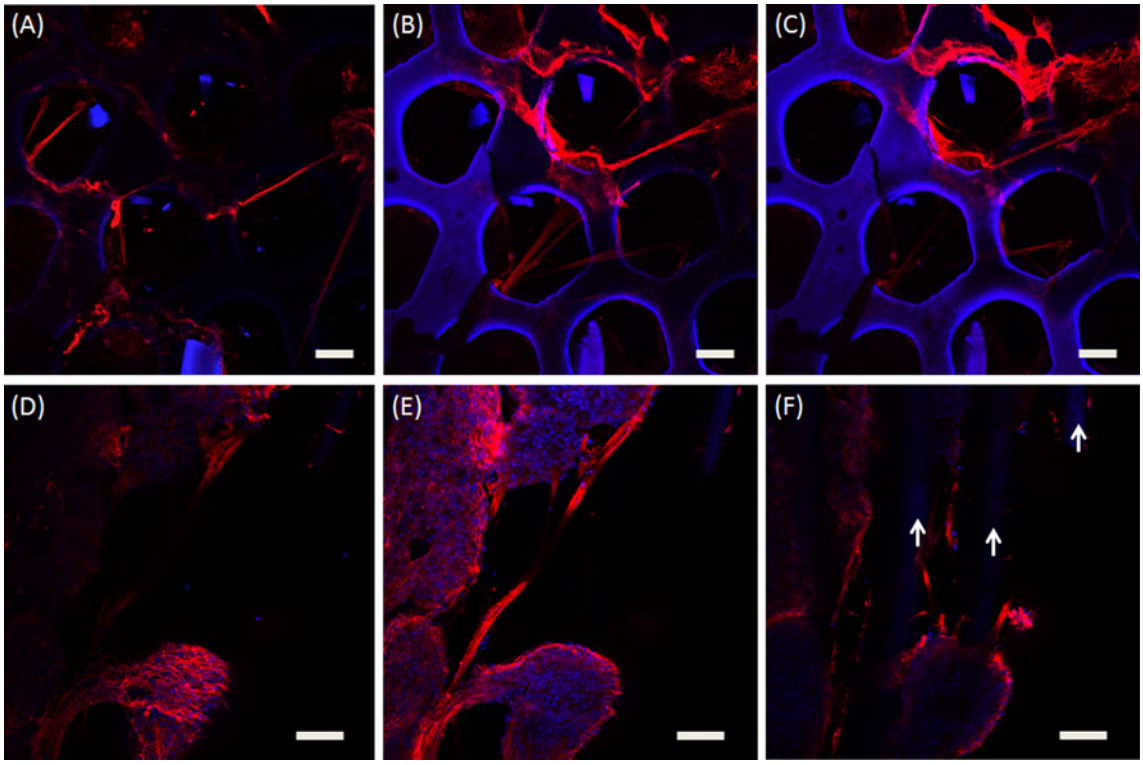

Fig. 4 Confocal images of the stiff PEGDA scaffold with hexagonal (**a**–**c**) and log-pile (**d**–**f**) architecture. Images selected from selected z-planes demonstrate the formation of neural connections in 3D labeled with Tuj1, a marker of early neurons. White arrows in (**f**) denotes the log-pile structure. Scale: 100 μm

the scaffold structure and through its porous spaces in three dimensions. Confocal stacks for both hexagonal (Fig. 4a–c) and log-pile (Fig. 4d–f) scaffolds demonstrate formation of early neurons as they label for Tuj1. The neurons assumed complex 3D morphologies with high neural connections across and into the hexagonal geometry, and have the potential to be used as a new platform for neurobiological investigations.

For soft PEGDA, cells were immunoreactive to both Tuj1 (green) and MAP2 (red) throughout the scaffold, although labeling of MAP2 was not very strong. Confocal stack (Fig. 5a–c) and 3D restructured image (Fig. 5d) both show 3D neurite formation at various z planes. A high resolution (40X z stack, Fig. 5e–g, Yellow color is because of merging of channels, red and green) also demonstrates formation of neurite structures near the hexagonal patterns. SEM images (Fig. 5h–k) demonstrates the scaffolds with multiple individual cells adhered to the side walls of the hexagonal scaffolds. Some parts of the scaffolds have collapsed and might be an SEM imaging artifact. Neurons within these scaffolds exhibit extensive 3D neurite outgrowth with expression of mature neuron-specific cytoskeletal markers. Synthetic PEGDA biomaterial provides a clean slate to graft any number of biomolecules such as RGD peptides, growth factors and biomolecules necessary for growth and differentiation. We chose the minimum size of the scaffold strut to be about 100 microns, which facilitates efficient nutrient/oxygen exchange, vascularization and tissue ingrowth in the scaffold, which has been problematic with scaffolds with small pore sizes. The scaffolds made of either PEGDA or GelMA are optically transparent and therefore, are compatible with standard microscopy techniques. High-stiffness PEDGA scaffolds were chosen for ease of handling the 3D culture system. They could survive for long periods of time, enabling drug testing, screening and development of diagnostic cell-based technologies. Non-biodegradable PEGDA may also be used to establish stable and long-term 3D cultures necessary for differentiation and enrichment of neuronal subtypes.

We also used GelMA scaffolds to evaluate their potential as a culture system for neural cell adhesion and differentiation. Naturally derived gelatin based GelMA scaffolds does not need any synthetic adhesive peptide sequence to facilitate cell adhesion. Multi-layer GelMA scaffolds of hexagonal geometry were fabricated as shown in Fig. 6f. With biodegradable GelMA scaffolds, after culture for 3 weeks, neuronal projections formed 3D networks labeling both Tuj1 (green) and

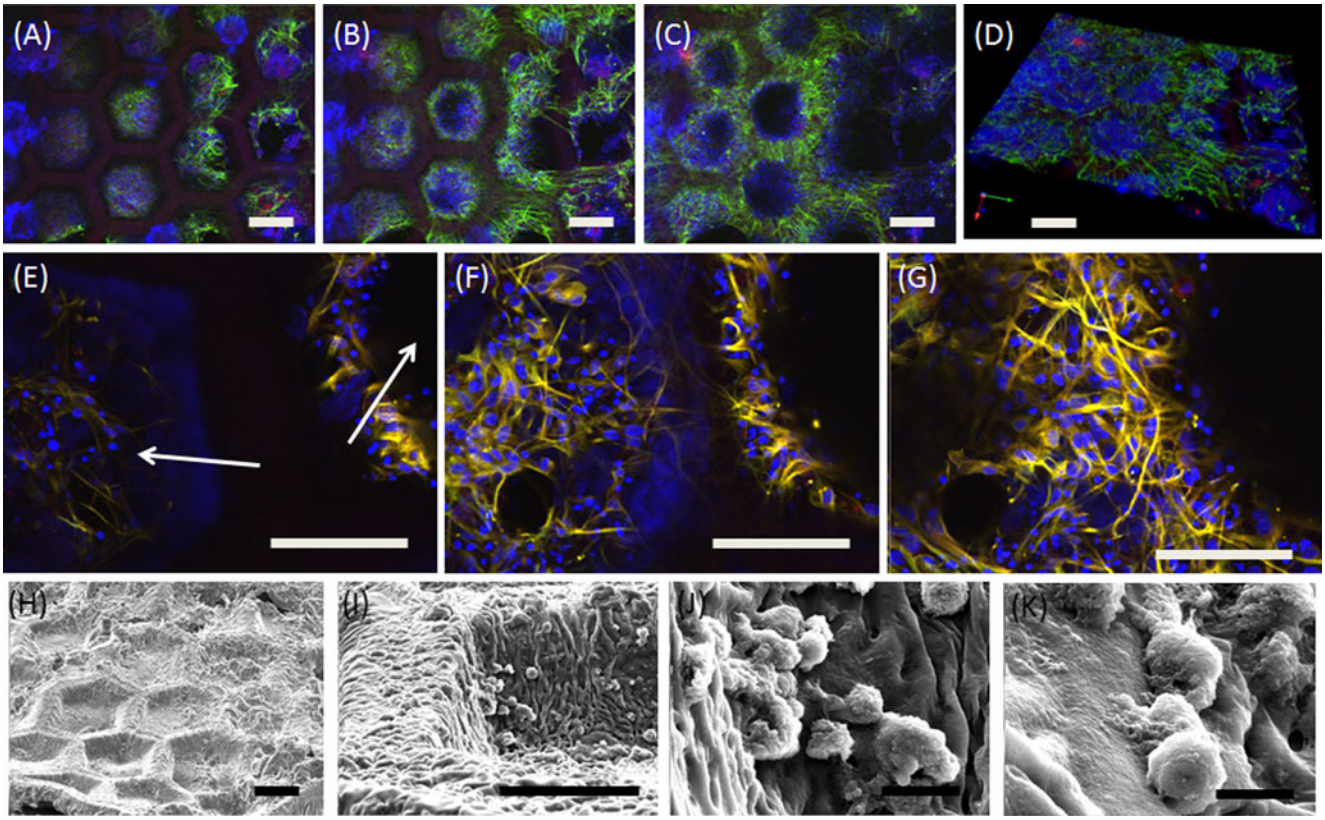

Fig. 5 Confocal images of soft PEGDA scaffold with hexagonal (**a**–**c**) geometry from selected z-sections labeled with Tuj1(green), MAP2 (red) and nucleus (DAPI-blue). (**d**) 3D reconstruction of the hexagonal scaffold. (**e**–**g**) High resolution image of the soft PEGDA scaffolds show clusters of neural cells formatting 3D neural connections between two hexagonal geometries. White arrows in (**e**) denote the hexagonal structure. (**h**–**k**) SEM images of the soft PEGDA scaffold. Scale: A-I= 100 μm; J,K=10 μm

MAP2 (red) across z planes (Fig. 6a–c). In these scaffolds, however, the hexagonal structure has almost completely degraded with only a couple of z planes showing a degraded hexagonal structure (See Inset in Fig. 6c). GelMA scaffolds for more than 4 weeks do not show any hexagonal geometry (Fig. 6d–e). Extensive neurite growth was evident under bright field microscopy by week 2, but the connections became rich with maturation of the culture. Neurons in GelMA scaffold assume 3D morphologies with extensive neurite extension in three dimensions, and express neuronal–specific microtube-associated protein MAP2 (red) and Tuj (green) with nuclear DAPI staining. One problem with GelMA cultures is the reduction of mechanical stability and difficulty in handling these scaffolds after three weeks of cell-culture. From optical images (Fig. 6f), it is clear that DMD-PP can fabricate complex hexagonal structure using GelMA, however, after 3–4 weeks, most of the scaffold geometry is completely degraded by the cells.

Two-dimensional culture systems have inherent limitations for engineering complex tissues and organoids (Vunjak-Novakovic and Scadden 2011). This is particularly relevant to the culture of human brain cells which are well known to extend long axonal processes in three dimensions in the normal brain with extensive intercellular interactions (Edelman and Keefer 2005). Development of standardized and robust methods for neuronal culture has been impeded by the sensitivity of neural differentiation intermediates to environmental cues and cell density causing heterogeneity and variability (Chambers et al. 2009). Our study was aimed at engineering scaffolds of well-defined geometrical shapes capable of supporting cell survival and enhancing intercellular connectivity of human neurons, with a long-term goal of developing a tissue engineered cell–scaffold constructs for phenotypic assays, drug validation and toxicity, as well as tissue engineering of complex multicellular neural organoids. DMD-PP fabricated scaffolds provide mechanical stability, structural guidance, and a matrix for cell integration with surrounding tissue. Scaffolds fabricated by DMD-PP provide a framework for the cells and tissue by customizing mechanical properties and internal geometries and thereby avoiding cell death to the lack of nutrients diffusing within the 3D environment. This work also highlights the automated high-throughput aspect of the

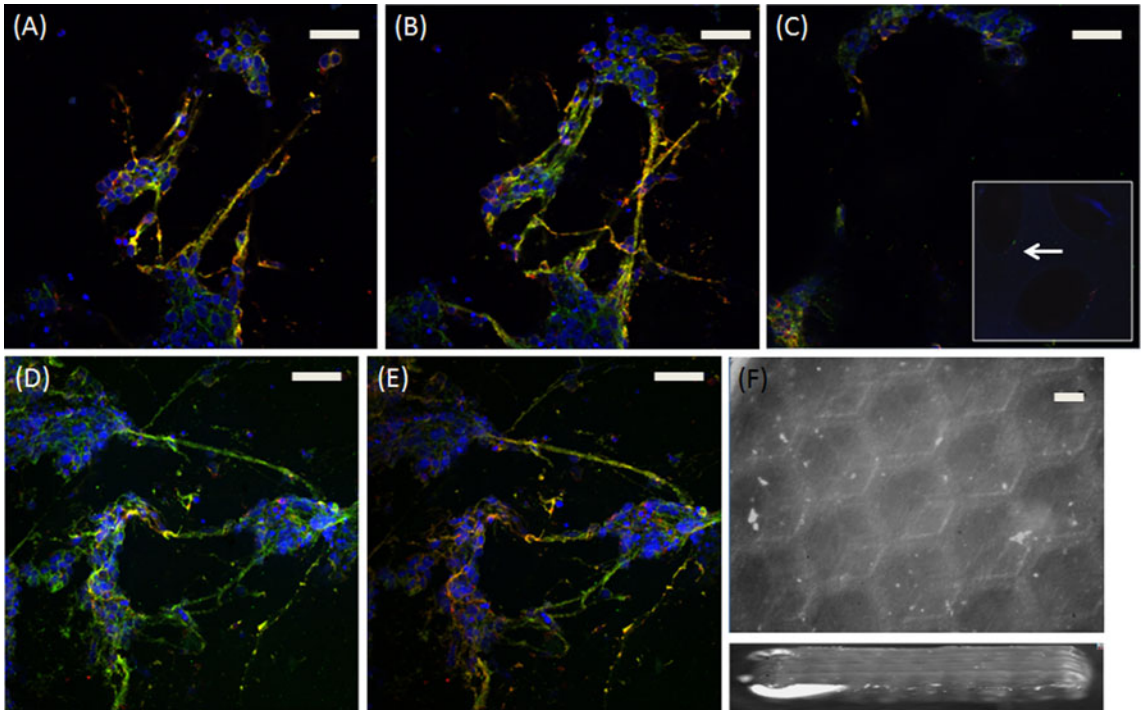

Fig. 6 Confocal z-stack images of gelatin methacrylate (GelMA) scaffolds with hexagonal (**a**–**c**) geometry labeled with Tuj1(green), MAP2 (red) and nucleus (blue). White arrows in inset (**c**) denote the degraded hexagonal structure after three-week of cell culture. (**d**–**e**) The hexagonal structure is not observed after four-week of culture. (**f**) Optical images of the GelMA scaffold with hexagonal structures before cell culture. Scale: 100 μm

scaffold fabrication process, to develop scaffold with standardized pore-sizes, internal geometries and mechanical properties using different biomaterials. This opens up possibility of orthogonally tuning singular aspects of fabrication (mechanical property, geometry etc.) without affecting other parameters (pore-sizes etc) and thus facilitating standardization of culture conditions for cell-based drug and toxicity screenings using neuronal derivatives from stem cells.

4 Conclusion

Our results demonstrate the use of a DMD-PP method for engineering 3D scaffolds of precisely defined geometries capable of supporting human neuronal cellular growth. This fully automated approach produced complex hexagonal and log-pile 3D constructs conducive to cell seeding and differentiation of neurospheres and growth of passaged neurons derived from human embryonic stem cells. Furthermore, interconnectivity and alignment of hexagonal pores facilitated 3D neurite connections in both synthetic PEDGA and naturally-derived GelMA scaffolds. Variation of the porous architecture and prepolymer concentration enabled tailoring the scaffold's mechanical properties. The combination of this microfabrication approach with photopolymerizable biomaterials may have implications in long-term human neural cell culture.

Acknowledgements The project described was supported in part by Award Number R01EB012597 from the National Institute of Biomedical Imaging And Bioengineering and grants (CMMI-1130894, CMMI-1120795) from the National Science Foundation. Thanks to Joseph Russo of Sanford-Burnham Imaging Core Facility for technical expertise. BT is funded by UCSD Dept. of Psychiatry NIH T32.

References

T.B. Bini, S. Gao, S. Wang, S. Ramakrishna, Poly(l-lactide-co-glycolide) biodegradable microfibers and electrospun nanofibers for nerve tissue engineering: an *in vitro* study. J. Mater. Sci. **41**(19), 6453–6459 (2006)

M.Z.A. Björn Carlberg, Nannmark Ulf, Liu Johan, H. Georg Kuhn, Electrospun polyurethane scaffolds for proliferation and neuronal differentiation of human embryonic stem cells. Biomed. Mater. **4** (4), 045004 (2009)

S.M. Chambers, C.A. Fasano, E.P. Papapetrou, M. Tomishima, M. Sadelain, L. Studer, Highly efficient neural conversion of human ES and iPS cells by dual inhibition of SMAD signaling. Nat. Biotechnol. **27**(3), 275–280 (2009)

P.L. Chandran, V. Barocas, Affine versus non-affine fibril kinematics in collagen networks: theoretical studies of network behavior. J. Biomech. Eng. **128**(2), 259–270 (2006)

L.P. Deleyrolle, B.A. Reynolds, Isolation, expansion, and differentiation of adult Mammalian neural stem and progenitor cells using the neurosphere assay. Methods Mol. Biol. **549**, 91–101 (2009)

D.B. Edelman, E.W. Keefer, A cultural renaissance: *in vitro* cell biology embraces three-dimensional context. Exp. Neurol. **192**(1), 1–6 (2005)

Y. Elkabetz, G. Panagiotakos, G. Al Shamy, N.D. Socci, V. Tabar, L. Studer, Human ES cell-derived neural rosettes reveal a functionally distinct early neural stem cell stage. Genes Dev. **22**(2), 152–165 (2008)

D.Y. Fozdar, P. Soman, W. LeeJin, L.-H. Han, S. Chen, Three-dimensional polymer constructs exhibiting a tunable negative poisson's ratio. Adv. Funct. Mater. (2011) In Press

R. Gauvin, Y.-C. Chen, J.W. Lee, P. Soman, P. Zorlutuna, J.W. Nichol et al., Microfabrication of complex porous tissue engineering scaffolds using 3D projection stereolithography. Biomaterials **33** (15), 3824–3834 (2012)

K. Gelse, E. Pöschl, T. Aigner, Collagens–structure, function, and biosynthesis. Adv. Drug Deliv. Rev. **55**(12), 1531–1546 (2003)

L.H. Han, G. Mapili, S. Chen, K. Roy, Projection microfabrication of three-dimensional scaffolds for tissue engineering. J Manuf Sci E–T ASME 2008 Apr;130(2) (2008)

J.B. Jensen, M. Parmar, Strengths and limitations of the neurosphere culture system. Mol. Neurobiol. **34**(3), 153–161 (2006)

A. Kunze, M. Giugliano, A. Valero, P. Renaud, Micropatterning neural cell cultures in 3D with a multi-layered scaffold. Biomaterials **32** (8), 2088–2098 (2011)

H.J. Lam, S. Patel, A. Wang, J. Chu, S. Li, *In vitro* regulation of neural differentiation and axon growth by growth factors and bioactive nanofibers. Tissue Eng. Part A **16**(8), 2641–2648 (2011)

H. Lee, G.A. Shamy, Y. Elkabetz, C.M. Schofield, N.L. Harrsion, G. Panagiotakos et al., Directed differentiation and transplantation of human embryonic stem cell-derived motoneurons. Stem Cells **25** (8), 1931–1939 (2007)

J. Lee, M.J. Cuddihy, N.A. Kotov, Three-dimensional cell culture matrices: state of the art. Tissue Eng. Part B Rev. **14**(1), 61–86 (2008)

S. Levenberg, N.F. Huang, E. Lavik, A.B. Rogers, J. Itskovitz-Eldor, R. Langer, Differentiation of human embryonic stem cells on three-dimensional polymer scaffolds. Proc. Natl. Acad. Sci. **100** (22), 12741–12746 (2003)

W. Li, W. Sun, Y. Zhang, W. Wei, R. Ambasudhan, P. Xia et al., Rapid induction and long-term self-renewal of primitive neural precursors from human embryonic stem cells by small molecule inhibitors. Proc. Natl. Acad. Sci. U. S. A. **108**(20), 8299–8304 (2011)

H. Liu, S.C. Zhang, Specification of neuronal and glial subtypes from human pluripotent stem cells. Cell Mol. Life Sci. **68**(24), 3995–4008 (2011)

W. Ma, W. Fitzgerald, Q.Y. Liu, T.J. O'Shaughnessy, D. Maric, H.J. Lin et al., CNS stem and progenitor cell differentiation into functional neuronal circuits in three-dimensional collagen gels. Exp. Neurol. **190**(2), 276–288 (2004)

M.C. Manzini, C.A. Walsh, What disorders of cortical development tell us about the cortex: one plus one does not always make two. Curr. Opin. Genet. Dev. **21**(3), 333–339 (2011)

G.P. Marshall 2nd, B.A. Reynolds, E.D. Laywell, Using the neurosphere assay to quantify neural stem cells *in vivo*. Curr. Pharm. Biotechnol. **8**(3), 141–145 (2007)

A. Pathak, S. Kumar, Biophysical regulation of tumor cell invasion: moving beyond matrix stiffness. Integr. Biol. **3**(4), 267–278 (2011)

J. Pedersen, M. Swartz, Mechanobiology in the third dimension. Ann. Biomed. Eng. **33**(11), 1469–1490 (2005)

A.L. Perrier, V. Tabar, T. Barberi, M.E. Rubio, J. Bruses, N. Topf et al., Derivation of midbrain dopamine neurons from human embryonic stem cells. Proc. Natl. Acad. Sci. U. S. A. **101**(34), 12543–12548 (2004)

D. Ren, J.D. Miller, Primary cell culture of suprachiasmatic nucleus. Brain Res. Bull. **61**(5), 547–553 (2003)

K. Sango, H. Saito, M. Takano, A. Tokashiki, S. Inoue, H. Horie, Cultured adult animal neurons and schwann cells give us new insights into diabetic neuropathy. Curr. Diabetes Rev. **2**(2), 169–183 (2006)

E. Shahbazi, S. Kiani, H. Gourabi, H. Baharvand., Electrospun nanofibrillar surfaces promote neuronal differentiation and function from human embryonic stem cells. Tissue Eng. Part A 2011/08/17 (2011)

R.F. Silva, A.S. Falcao, A. Fernandes, A.C. Gordo, M.A. Brito, D. Brites, Dissociated primary nerve cell cultures as models for assessment of neurotoxicity. Toxicol. Lett. **163**(1), 1–9 (2006)

I. Singec, R. Knoth, R.P. Meyer, J. Maciaczyk, B. Volk, G. Nikkhah et al., Defining the actual sensitivity and specificity of the neurosphere assay in stem cell biology. Nature methods **3**(10), 801–806 (2006)

P. Soman, J.W. Lee, A. Phadke, S. Varghese, S. Chen. Spatial tuning of negative and positive Poissonâ€™s ratio in a multi-layer scaffold. Acta Biomaterialia (0) (2012)

C. Storm, J.J. Pastore, F.C. MacKintosh, T.C. Lubensky, P.A. Janmey, Nonlinear elasticity in biological gels. Nature **435**(7039), 191–194 (2005)

G. Vunjak-Novakovic, D.T. Scadden, Biomimetic platforms for human stem cell research. Cell Stem Cell **8**(3), 252–261 (2011)

S.M. Willerth, K.J. Arendas, D.I. Gottlieb, S.E. Sakiyama-Elbert, Optimization of fibrin scaffolds for differentiation of murine embryonic stem cells into neural lineage cells. Biomaterials **27** (36), 5990–6003 (2006)

J.P. Winer, S. Oake, P.A. Janmey, Non-linear elasticity of extracellular matrices enables contractile cells to communicate local position and orientation. PLoS One **4**(7), e6382 (2009)

F. Yang, R. Murugan, S. Wang, S. Ramakrishna, Electrospinning of nano/micro scale poly(L-lactic acid) aligned fibers and their potential in neural tissue engineering. Biomaterials **26**(15), 2603–2610 (2005)

S.C. Zhang, Neural subtype specification from embryonic stem cells. Brain Pathol. **16**(2), 132–142 (2006)